

CLINICAL REPORT **OPEN ACCESS**

Loss-of-Function *CARS1* Variants in a Patient With Microcephaly, Developmental Delay, and a Brittle Hair Phenotype

Christina Del Greco¹  | Molly E. Kuo^{1,2,3} | Desiree E. C. Smith⁴ | Marisa I. Mendes⁴ | Gajja S. Salamons⁴ | Marek Nemcovic⁵ | Rebeka Kodrikova⁵ | Sergej Sestak⁵  | Malina Stancheva⁶ | Anthony Antonellis^{1,2,7}

¹Department of Human Genetics, University of Michigan Medical School, Ann Arbor, Michigan, USA | ²Cellular and Molecular Biology Program, University of Michigan Medical School, Ann Arbor, Michigan, USA | ³Medical Scientist Training Program, University of Michigan Medical School, Ann Arbor, Michigan, USA | ⁴Laboratory Genetic Metabolic Diseases, Amsterdam UMC, University of Amsterdam, Amsterdam, the Netherlands | ⁵Institute of Chemistry, Department of Glycobiology, Slovak Academy of Sciences, Bratislava, Slovakia | ⁶Medico-Dental Center Mediva, Sofia, Bulgaria | ⁷Department of Neurology, University of Michigan Medical School, Ann Arbor, Michigan, USA

Correspondence: Sergej Sestak (sergej.sestak@savba.sk) | Malina Stancheva (malinastancheva@yahoo.com) | Anthony Antonellis (antonell@umich.edu)

Received: 12 October 2024 | **Revised:** 17 January 2025 | **Accepted:** 4 February 2025

Funding: C.D. is supported by the Michigan Pre-doctoral Training in Genetics Program (T32GM149391) and an NIH National Research Service Award from the National Institute for Child Health and Human Development (F31HD111131). M.E.K. is supported by the NIH Medical Scientist Training Program Training Grant (T32GM007863), the NIH Cellular and Molecular Biology Training Grant (T32GM007315), and an NIH National Research Service Award from the National Institute of Neurological Disorders and Stroke (F31NS113515). A.A. is supported by a grant from the National Institute of General Medical Sciences (GM136441). This publication was supported in part by the Operational Program Integrated Infrastructure for the project ITMS: 313021Y920, co-financed by the European Regional Development Fund.

ABSTRACT

Background: Mutations in cysteinyl-tRNA synthetase (*CARS1*) have been implicated in a multisystem disease including microcephaly, developmental delay, and brittle hair and nail phenotypes.

Methods: Here, we present a patient with hepatopathy, hypothyroidism, short stature, developmental delay, microcephaly, muscular hypotonia, brittle hair, and ataxia. The patient underwent exome sequencing to identify potentially pathogenic genetic variants. In addition, identified variants were assessed using yeast complementation assays to determine functional consequences.

Results: Exome sequencing determined that the patient is compound heterozygous for p.Arg341His and p.Arg370Trp *CARS1*. Yeast complementation assays showed that the p.Arg341His variant has a hypomorphic effect and that the p.Arg370Trp variant causes a complete loss-of-function effect.

Conclusion: This study is the second report of pathogenic *CARS1* variants and expands the allelic and phenotypic heterogeneity of *CARS1*-associated disease.

1 | Background

Aminoacyl-tRNA synthetases (ARSs) are essential enzymes that charge tRNA with cognate amino acids (Antonellis and Green 2008). There are 37 human ARSs—all nuclear-encoded—that are responsible for charging tRNA in the cytoplasm and the mitochondria (Antonellis and Green 2008).

All 37 ARSs have been associated with recessive, multisystem phenotypes that often affect the central nervous system (Kuo and Antonellis 2020). Variants in ARS-associated recessive disease have loss-of-function effects on protein function (Meyer-Schuman and Antonellis 2017). Mutations in cysteinyl-tRNA synthetase (*CARS1*; MIM: 123859), which encodes the *CARS1* protein that charges tRNA with cysteine in the cytoplasm, were

This is an open access article under the terms of the [Creative Commons Attribution-NonCommercial-NoDerivs](https://creativecommons.org/licenses/by-nc-nd/4.0/) License, which permits use and distribution in any medium, provided the original work is properly cited, the use is non-commercial and no modifications or adaptations are made.

© 2025 The Author(s). *Molecular Genetics & Genomic Medicine* published by Wiley Periodicals LLC.

previously implicated in a multisystem recessive disease that includes microcephaly, developmental delay, and brittle hair and nail phenotypes (Kuo et al. 2019). Here, we present a patient with biallelic *CARS1* variants—one previously identified by Kuo et al. and one previously unreported—who presents with hepatopathy, hypothyroidism, short stature, developmental delay, microcephaly, muscular hypotonia, brittle hair, and ataxia.

2 | Methods

2.1 | Clinical Methods

The proband was assessed using family history, disease history, and consultation with specialists. Psychological assessment methods included Denver II screening, developmental profile 3 (DP-3) testing, Reynolds Intellectual Assessment Scales (RIAS-2) assessment, and Clinical Assessment of Behavior (CAB). Radiological assessment methods included radiography of the wrist, echography of the abdomen, echocardiography, and brain magnetic resonance imaging (MRI). Neuropsychological assessment methods included electroencephalogram (EEG) and echocardiography. The proband also underwent otoacoustic emission (OAE) testing and biochemical and hormonal analysis; specific analyses are listed in the supplemental clinical data. Informed consent was obtained from the proband's parents.

2.2 | Exome Sequencing

Whole-exome sequencing (WES) was performed at the Centre for Mendelian Genomics at the University Medical Centre Ljubljana, Slovenia. Sequencing was performed on DNA from venous blood, and data was processed through PhenoSystems by GensearchNGS. Sanger sequencing was performed to confirm WES results.

2.3 | Sanger Sequencing

The mutations identified by WES were confirmed by Sanger sequencing of the genomic DNA isolated from blood of the patient. The primer pairs used for the amplification of 1.4 kb fragment were designed: the forward primer used was 5'-CTGGGTCAACACCAGAATC-3' and the reverse primer was 5'-GCACCTGACAAGGGGACTC-3'. DNA amplification was performed using GoTaq DNA Polymerase (Promega, Madison, Wisconsin). The following conditions were used for amplification: 1 cycle of 95°C for 2 min, followed by 35 cycles of 95°C for 30s, 55°C for 30s, 72°C for 90s, and a final extension at 72°C for 5 min. Amplified PCR product was purified using Wizard SV Gel and PCR Clean-Up System (Promega) and sequenced.

2.4 | Multiple-Species Alignment

The Clustal Omega program was used to align *CARS1* protein sequences from multiples species. The following GenBank accession numbers were used: human (*Homo sapiens*, NP_001742.1); mouse (*Mus musculus*, NP_001239522.1); zebrafish (*Danio rerio*, NP_001112372.1); worm (*Caenorhabditis*

elegans, NP_001293288.1); yeast (*Saccharomyces cerevisiae*, NP_014152.1); and bacteria (*Escherichia coli*, CAU96413.1).

2.5 | Enzyme Analysis

Aminoacylation activity of *CARS1* was assayed in fibroblast lysates of the patient and a control cell line. In addition, *GARS1* activity was simultaneously measured as an internal control. In brief, assays were performed at 37°C in reaction buffer (50 mmol/L Tris buffer [pH 7.5], 12 mmol/L MgCl₂, 25 mol/L KCl), 1 mg/mL bovine serum albumin, 0.5 mmol/L spermine, 1 mmol/L ATP, 0.2 mmol/L yeast total tRNA, 1 mmol/L dithiothreitol, and 0.3 mM [¹³C₄, ¹⁵N] cysteine and [D₂] glycine. The reaction was terminated with trichloroacetic acid (TCA). After reaction termination and washing, ammonia was added to release [¹³C₄, ¹⁵N] cysteine and [D₂] glycine from tRNA molecules. [¹³C₂, ¹⁵N] glycine was added as an internal standard. Labeled amino acids were quantified by liquid chromatography–tandem mass spectrometry (LC–MS/MS).

2.6 | Yeast Complementation Assays

Yeast complementation assays to study the functional consequences of *CARS1* variants were performed as previously described (Kuo et al. 2019). The p.Arg370Trp variant was introduced into the *CARS1* open reading frame using QuikChange II XL Site-Directed Mutagenesis Kit (Agilent; Table S1) in the pDONR221 vector. After mutagenesis, the *CARS1* open reading frame was fully sequenced to confirm the presence of only the desired variant and then recombined into the pYY1 expression vector bearing the *LEU2* gene (Chien et al. 2014) using Gateway cloning (Invitrogen). The p.Arg341His *CARS1* pYY1 expression construct was generated in previous studies (Kuo et al. 2019). These constructs were transformed into a haploid Δ *CRS1* yeast strain with viability maintained using an exogenous copy of *CRS1* on the pRS316 maintenance vector containing the *URA3* gene (Kuo et al. 2019). Transformants were grown on media lacking both leucine and uracil to select for colonies containing both the maintenance and experimental plasmids. Individual colonies were grown to saturation, shaking at 275 rpm at 30°C for 2 days. A 1 mL of saturated culture was then concentrated by centrifuging at 15,000 rpm for 1 min and resuspending in 50 μ L of Ultrapure water. A 10 μ L of each concentrated culture was spotted (undiluted or diluted 1:10 or 1:100 in water) on plates containing 0.1% 5-FOA to select for spontaneous loss of the maintenance vector (Boeke et al. 1984). Plates were incubated at 30°C and yeast growth was visually inspected after 3–5 days. For each variant, two independently-generated expression constructs were tested across three experimental replicates, and two to four colonies were spotted for analysis, per experiment.

2.7 | Yeast Spot Quantification

Yeast growth was quantified using ImageJ based on the protocol described in Petropavlovskiy et al. 2020 (Petropavlovskiy et al. 2020). Background was subtracted using the “subtract background” function by setting the “rolling ball radius” to spot diameter + 20 and selecting “sliding paraboloid.” Image

brightness was adjusted using brightness/contrast set to “auto.” To quantify, gray value densitometry measures were taken for four background samples and one for each spot at the undiluted concentration. Both the background and the empty vector control measures were subtracted from each wild-type and variant measurement, and then each measurement was normalized to the wild-type gray value. Replicates were averaged to get final values. Data was analyzed using a one-way ANOVA and Tukey HSD tests to calculate significance between samples.

3 | Results

3.1 | Clinical Data

The proband (Figure 1A) is of Bulgarian descent and was born at 38 weeks gestation to unaffected parents. He presented with intrauterine growth restriction and fetal hypotrophy at 36 weeks gestation. He was born at slightly below average weight and

height (2.45 kg, 47 cm, ≤ 5 percentile). At 3 months, he had not gained any weight and was diagnosed with failure to thrive, hypoglycemia, hepatomegaly, and elevated transaminases, and nasogastric tube feedings were initiated from ages 1 through 3 years. At 1 year of age, he had EEG changes that prompted treatment with levetiracetam until the age of 3. He began to walk at 2 years and 6 months, at which point he could speak simple words but could not form sentences. He presented with developmental delay and on physical examination at 2 years and 9 months he had short stature, facial dysmorphisms (bitemporal narrowing, midface hypoplasia, downslating palpebral fissures, hypotelorism, blue sclerae, anteverted concha, low nasal base, divergent strabismus), brittle hair (Figure 1B), positive bilateral Babinski reflexes, and ataxic gait. Laboratory findings were notable for elevated liver transaminases, dyslipidemia, hypoalbuminemia, hypoglycemia, and hypothyroidism; although, at 7 years of age transaminases are normal. Although initial brain imaging performed at 1 year of age indicated potential abnormalities, MRI performed at 4 years and 5 months showed no

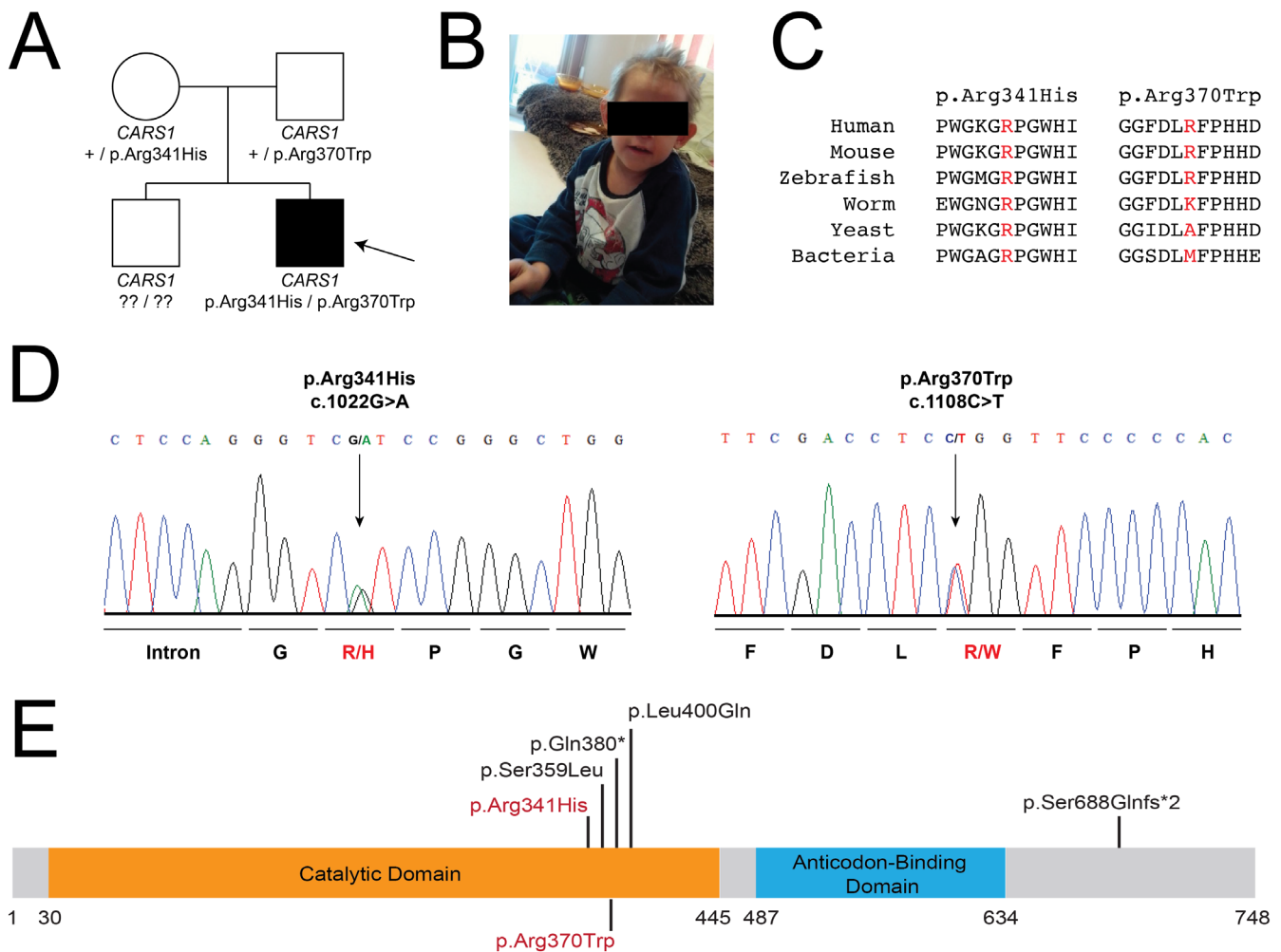


FIGURE 1 | *CARS1* variants found in proband. (A) Pedigree showing inheritance of the *CARS1* alleles. Squares represent males, circles represent females, and the filled square indicates the affected individual. The arrow indicates the proband. Genotypes are below each individual and question marks indicate unknown genotypes. (B) Photograph showing brittle hair phenotype of the proband. (C) Multiple-species alignment of *CARS1* amino-acid sequences. The protein annotation of the variant is above, the species names are on the left, and the affected residues are highlighted in red. (D) Sanger sequencing of proband gDNA validating the missense variants found by WES. (E) Diagram of *CARS1* protein domains with previously described variants shown at the top of the figure and the newly described variant shown at the bottom of the figure. Variants identified in the proband are in red.

TABLE 1 | *CARS1* patient variant allele frequency.

Nucleotide change ^a	Amino acid change ^b	Detection in gnomAD ^c	Minor allele frequency	# Homozygotes in gnomAD
c.1022G>A	p.Arg341His	26/599,544	0.000043	0
c.1108C>T	p.Arg370Trp	5/1,526,966	0.000003	0

^aHuman nucleotide positions correspond to NM_001751.6.

^bHuman amino acid positions correspond to NP_001742.1.

^cgnomad.broadinstitute.org v4.0.0.

brain abnormalities. Abdominal ultrasound showed lesions on the liver—potentially hemangiomas—and echocardiography ordered due to previous heart murmur showed membranous ventricular septal defect, which has since closed. At 4 years and 9 months of age, the proband was treated with L-thyroxin, ursodeoxycholic acid, glutathione spray, and vitamin C. By 6 years and 9 months of age, he had two generalized tonic-clonic seizures, for which he was treated with levetiracetam; EEG was normal. As of March 2024, he was 7 years old, 13.4 kg (−3 SDS), 102.5 cm tall (−4.49 SDS), and treated with L-thyroxin, ursodeoxycholic acid, and levetiracetam. At present, the proband has delayed speech development and fine motor skills. Reflexes are normal, and neurological assessment shows no measurable residual disease. Additional clinical details can be found in the supplement.

3.2 | Variant Data

The proband has a normal male karyotype (46, XY). He underwent whole-exome sequencing using DNA isolated from lymphocytes in venous blood. WES analysis found biallelic variants in the *CARS1* gene: c.1022G>A (p.Arg341His) and c.1108C>T (p.Arg370Trp) (Figure 1A,D). Sanger sequencing confirmed the presence of both variants in the heterozygous state in the proband (Figure 1D). Sequencing of the parents revealed that the mother is heterozygous for the c.1022G>A allele and the father is heterozygous for the c.1108C>T allele. The proband's brother, who has cryptorchidism and refractory eye anomalies, has not yet undergone genetic analysis (Figure 1A). We assessed the evolutionary conservation of these variants. The p.Arg341 residue is conserved among all analyzed species, and the p.Arg370 residue is conserved among human, mouse, and zebrafish (Figure 1C). Both variants fall within the catalytic domain of the *CARS1* protein (Figure 1D). The frequency of these variants in the general population was assessed using the gnomAD database (Table 1) (Karczewski et al. 2020). The p.Arg341His variant is present in gnomAD at a low frequency (26/599,544), as is the p.Arg370Trp variant (5/1,526,966). None of these variants were found in the homozygous state. These data indicate that these variants occur at amino-acid residues that are potentially important for enzyme function.

3.3 | Functional Data

To determine the functional consequences of the *CARS1* variants described in this study, we assessed the enzyme activity of the *CARS1* protein in patient fibroblast lysates. The average *CARS1*

aminoacylation activity was decreased in the patient cells compared to controls (37%), similar to levels previously shown in Kuo et al. (Kuo et al. 2019); however, there was significant variability in the samples. *GARS1* activity, determined simultaneously, was similar to the control activity (80% of control) (Figure S1).

We next tested the ability of wild-type or mutant human *CARS1* to complement deletion of *CRS1* in yeast; *CRS1* encodes the yeast ortholog of *CARS1*. We used a haploid yeast strain with endogenous *CRS1* deleted and with viability maintained via a maintenance vector harboring *CRS1* and *URA3* generated in a previous study (Kuo et al. 2019). Yeast transformations were performed in replicates corresponding to patient genotypes. Yeast transformed with an empty plasmid did not grow, confirming that *CRS1* is an essential gene. Wild-type human *CARS1* supported yeast growth, indicating that human *CARS1* is able to complement the loss of yeast *CRS1*. The p.Arg341His *CARS1* variant supported yeast growth, but not equally to wild-type *CARS1* (Figure 2A,B), indicating that p.Arg341His *CARS1* is a hypomorphic allele in this model as previously demonstrated (Kuo et al. 2019). The p.Arg370Trp *CARS1* variant did not support any yeast growth (Figure 2A,B), indicating that p.Arg370Trp *CARS1* is a complete loss-of-function allele in this model. Spots at the undiluted concentration taken from day 3 images were quantified to measure yeast growth compared to wild-type across all replicates, which supports the observations that p.Arg341His is hypomorphic ($p_{\text{adj}} < 0.0001$) and that p.Arg370Trp causes a loss-of-function effect ($p_{\text{adj}} < 0.0001$) in this system (Figure 2B).

4 | Discussion

Here we present a patient with biallelic *CARS1* variants and a multisystem disease including hepatopathy, hypothyroidism, short stature, developmental delay, microcephaly, muscular hypotonia, brittle hair, and ataxia. Functional data supports a partial loss-of-function effect for p.Arg341His *CARS1*, as previously demonstrated (Kuo et al. 2019), and a complete loss-of-function effect for p.Arg370Trp *CARS1*. Although enzyme analysis did not show any statistically significant differences in *CARS1* aminoacylation function between patient fibroblasts and control cells due to variability between replicates, the average enzyme activity was decreased in patient fibroblasts compared to controls. Further analysis is required to interrogate if the mutant *CARS1* proteins are defective in aminoacylation.

This study expands both the clinical and genotypic heterogeneity of *CARS1*-associated disease. As described in previous *CARS1* patients, the proband presents with brittle hair, which has also been

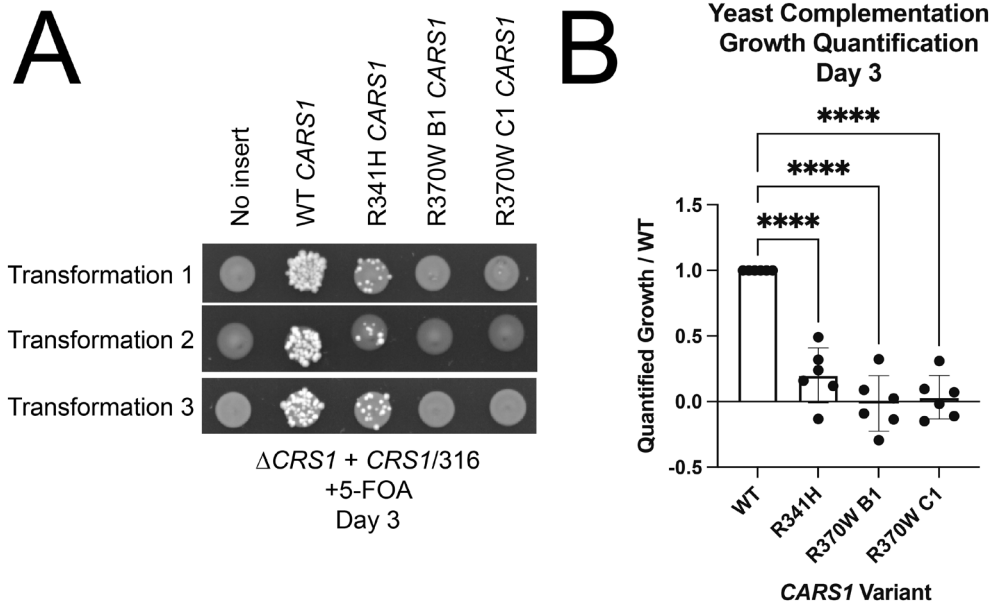


FIGURE 2 | *CARS1* variants cause a loss-of-function effect in yeast complementation assays. (A) Representative yeast complementation data from three separate transformations showing yeast transformed with the pYY1 yeast expression construct containing either no insert, wild-type *CARS1*, p.Arg341His *CARS1*, or one of two independently generated p.Arg370Trp *CARS1* constructs. Yeast cells were plated on 5-FOA and images show undiluted spots from each transformation. (B) Quantification of all replicates (one-way ANOVA $p < 0.0001$) demonstrates decreased growth with the p.Arg341His variant (Tukey HSD between wild-type and p.Arg341His; **** = $p_{\text{adj}} < 0.0001$) and the p.Arg370Trp variant (Tukey HSD between wild-type and each independent p.Arg370Trp construct; **** = $p_{\text{adj}} < 0.0001$).

TABLE 2 | Aminoacyl-tRNA synthetases with related clinical phenotypes.

Clinical phenotype	Associated ARSs
Dyslipidemia	<i>FARSA</i> (Krenke et al. 2019)
Elevated liver transaminases	<i>FARSA</i> (Krenke et al. 2019), <i>FARSB</i> (Antonellis et al. 2018; Xu et al. 2018), <i>IARSI</i> (Fuchs et al. 2019), <i>KARSI</i> (Fuchs et al. 2019), <i>LARSI</i> (Fuchs et al. 2019; Lenz et al. 2020), <i>MARSI</i> (Rips et al. 2018), <i>QARSI</i> (Fuchs et al. 2019), <i>YARSI</i> (Zeiad et al. 2021; Williams et al. 2019)
Hypoalbuminemia	<i>FARSA</i> (Krenke et al. 2019; Guo et al. 2023; Charbit-Henrion et al. 2022; Schuch et al. 2021), <i>FARSB</i> (Antonellis et al. 2018; Xu et al. 2018; Zadjali et al. 2018), <i>IARSI</i> (Fuchs et al. 2019), <i>KARSI</i> (Fuchs et al. 2019), <i>LARSI</i> (Fuchs et al. 2019; Lenz et al. 2020), <i>MARSI</i> (Rips et al. 2018), <i>YARSI</i> (Zeiad et al. 2021; Williams et al. 2019)
Hypoglycemia	<i>FARSB</i> (Antonellis et al. 2018), <i>LARSI</i> (Fuchs et al. 2019), <i>YARSI</i> (Zeiad et al. 2021; Williams et al. 2019)
Hypothyroidism	<i>FARSA</i> (Krenke et al. 2019; Guo et al. 2023), <i>FARSB</i> (Xu et al. 2018), <i>MARSI</i> (Rips et al. 2018), <i>YARSI</i> (Zeiad et al. 2021)

described in patients with *AARSI*- and *MARSI*-associated trichothiodystrophy (Kuo et al. 2019; Botta et al. 2021). Additionally, the proband presents with other phenotypes described in *CARS1* patients, including developmental delay, failure to thrive, seizures, and liver dysfunction (Kuo et al. 2019). Other phenotypes observed in this case, while not previously observed in *CARS1* patients, have been observed in patients with biallelic variants in other tRNA synthetases (Table 2). It is currently unclear what leads to differential phenotypes between the proband and previously reported cases of *CARS1*-associated disease. In addition, further investigation is required into why the brittle hair phenotype currently remains unique to *CARS1* patients.

In conclusion, our data support an expansion of the allelic and phenotypic heterogeneity of *CARS1*-associated recessive disease consistent with phenotypes found in other ARS-associated recessive multisystem disease, and supports the hypothesis that a depletion in ARS function leads to the recessive disease phenotypes.

Author Contributions

C.D.G. contributed to study conceptualization and methodology, data collection, analysis, and visualization, and writing the original draft of the manuscript. M.E.K., D.E.C.S., M.I.M., M.N., and R.K. contributed to the methodology, data collection, and analysis. M.S. performed the

clinical assessment of the proband and manuscript editing. G.S.S. and S.S. contributed to study conceptualization, data analysis, editing, and supervision. A.A. contributed to study conceptualization, data analysis, and visualization, writing the original draft, and study supervision. All authors read, provided feedback on, and approved the final manuscript.

Acknowledgements

We thank the family for participation in this study.

Consent

Informed consent was obtained from the proband's parents.

Conflicts of Interest

The authors declare no conflicts of interest.

Data Availability Statement

The data that support the findings of this study are available from the corresponding authors upon reasonable request.

References

- Antonellis, A., and E. D. Green. 2008. "The Role of Aminoacyl-tRNA Synthetases in Genetic Diseases." *Annual Review of Genomics and Human Genetics* 9: 87–107.
- Antonellis, A., S. N. Oprescu, L. B. Griffin, A. Heider, A. Amalfitano, and J. W. Innis. 2018. "Compound Heterozygosity for Loss-of-Function FARSB Variants in a Patient With Classic Features of Recessive Aminoacyl-tRNA Synthetase-Related Disease." *Human Mutation* 39, no. 6: 834–840.
- Boeke, J. D., F. LaCroute, and G. R. Fink. 1984. "A Positive Selection for Mutants Lacking Orotidine-5'-Phosphate Decarboxylase Activity in Yeast: 5-Fluoro-Orotic Acid Resistance." *Molecular & General Genetics* 197, no. 2: 345–346.
- Botta, E., A. F. Theil, A. Raams, et al. 2021. "Protein Instability Associated With AARS1 and MARS1 Mutations Causes Trichothiodystrophy." *Human Molecular Genetics* 30, no. 18: 1711–1720.
- Charbit-Henrion, F., R. Goguyer-Deschaumes, K. Borensztajn, et al. 2022. "Systemic Inflammatory Syndrome in Children With FARSA Deficiency." *Clinical Genetics* 101, no. 5–6: 552–558.
- Chien, C. I., Y. W. Chen, Y. H. Wu, C. Y. Chang, T. L. Wang, and C. C. Wang. 2014. "Functional Substitution of a Eukaryotic Glycyl-tRNA Synthetase With an Evolutionarily Unrelated Bacterial Cognate Enzyme." *PLoS One* 9, no. 4: e94659.
- Fuchs, S. A., I. F. Schene, G. Kok, et al. 2019. "Aminoacyl-tRNA Synthetase Deficiencies in Search of Common Themes." *Genetics in Medicine* 21, no. 2: 319–330.
- Guo, R., Y. Chen, X. Hu, et al. 2023. "Phenylalanyl-tRNA Synthetase Deficiency Caused by Biallelic Variants in FARSA Gene and Literature Review." *BMC Medical Genomics* 16, no. 1: 245.
- Karczewski, K. J., L. C. Francioli, G. Tiao, et al. 2020. "The Mutational Constraint Spectrum Quantified From Variation in 141,456 Humans." *Nature* 581, no. 7809: 434–443.
- Krenke, K., K. Szczałuba, T. Bielecka, et al. 2019. "FARSA Mutations Mimic Phenylalanyl-tRNA Synthetase Deficiency Caused by FARSB Defects." *Clinical Genetics* 96, no. 5: 468–472.
- Kuo, M. E., and A. Antonellis. 2020. "Ubiquitously Expressed Proteins and Restricted Phenotypes: Exploring Cell-Specific Sensitivities to Impaired tRNA Charging." *Trends in Genetics* 36, no. 2: 105–117.

Kuo, M. E., A. F. Theil, A. Kievit, et al. 2019. "CysteinyI-tRNA Synthetase Mutations Cause a Multi-System, Recessive Disease That Includes Microcephaly, Developmental Delay, and Brittle Hair and Nails." *American Journal of Human Genetics* 104, no. 3: 520–529.

Lenz, D., D. E. C. Smith, E. Crushell, et al. 2020. "Genotypic Diversity and Phenotypic Spectrum of Infantile Liver Failure Syndrome Type 1 due to Variants in LARS1." *Genetics in Medicine* 22, no. 11: 1863–1873.

Meyer-Schuman, R., and A. Antonellis. 2017. "Emerging Mechanisms of Aminoacyl-tRNA Synthetase Mutations in Recessive and Dominant Human Disease." *Human Molecular Genetics* 26, no. R2: R114–R127.

Petrovavlovskiy, A. A., M. G. Tauro, P. Lajoie, and M. L. Duennwald. 2020. "A Quantitative Imaging-Based Protocol for Yeast Growth and Survival on Agar Plates." *STAR Protocols* 1, no. 3: 100182.

Rips, J., R. Meyer-Schuman, O. Breuer, et al. 2018. "MARS Variant Associated With Both Recessive Interstitial Lung and Liver Disease and Dominant Charcot-Marie-Tooth Disease." *European Journal of Medical Genetics* 61, no. 10: 616–620.

Schuch, L. A., M. Forstner, C. K. Rapp, et al. 2021. "FARS1-Related Disorders Caused by Bi-Allelic Mutations in Cytosolic Phenylalanyl-tRNA Synthetase Genes: Look Beyond the Lungs!" *Clinical Genetics* 99, no. 6: 789–801.

Williams, K. B., K. W. Brigatti, E. G. Puffenberger, et al. 2019. "Homozygosity for a Mutation Affecting the Catalytic Domain of Tyrosyl-tRNA Synthetase (YARS) Causes Multisystem Disease." *Human Molecular Genetics* 28, no. 4: 525–538.

Xu, Z., W. S. Lo, D. B. Beck, et al. 2018. "Bi-Allelic Mutations in Phe-tRNA Synthetase Associated With a Multi-System Pulmonary Disease Support Non-Translational Function." *American Journal of Human Genetics* 103, no. 1: 100–114.

Zadjali, F., A. Al-Yahyaee, M. Al-Nabhani, et al. 2018. "Homozygosity for FARSB Mutation Leads to Phe-tRNA Synthetase-Related Disease of Growth Restriction, Brain Calcification, and Interstitial Lung Disease." *Human Mutation* 39, no. 10: 1355–1359.

Zeidi, R., E. C. Ferren, D. D. Young, et al. 2021. "A Novel Homozygous Missense Mutation in the YARS Gene: Expanding the Phenotype of YARS Multisystem Disease." *Journal of the Endocrine Society* 5, no. 2: bvaa196.

Supporting Information

Additional supporting information can be found online in the Supporting Information section.